CHAPTER 5

Experimental Studies

"In many respects the practice of vibration testing is more of an art than a science."
Maia *et al.* (1997)

5. EXPERIMENTAL STUDIES

The majority of the effort will be devoted to the determination of harmonic forces, since all other forms of excitation, be they transient, periodic or random, may be represented as a Fourier series. The likelihood of being able to determine these forces will depend on the success obtained for the harmonic case. The first part of each section describes the experimental setup, which is followed by the issues relating to the measurement process and finally concludes with the results and conclusions drawn from the study.

5.1 SINGLE HARMONIC FORCE: FREE-FREE BEAM

This section presents the first attempt to apply the previously derived theory to determine a single harmonic force on a free-free beam.

5.1.1 Details of the Experimental Set-up

The test piece consisted of an aluminium beam with the same geometrical dimensions as the beam considered in the FEA. The beam was discretised with eleven equally spaced node points, each constituted a potential sensor location, as depicted in Figure 5.1.

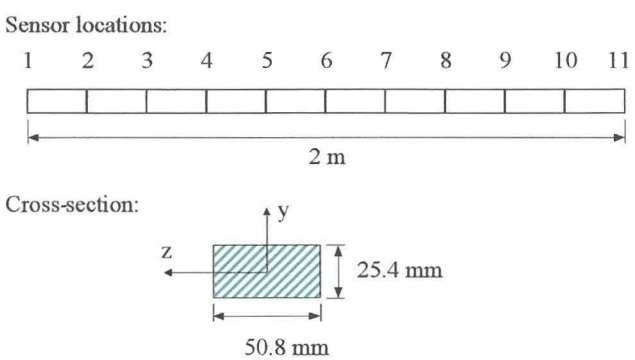

Figure 5.1 – Free-free aluminum beam and response locations

The beam was suspended on very soft elastic bands to approximate free-free boundary conditions. This type of suspension causes the theoretical 0 Hz Rigid Body Modes (RBM) to shift to slightly higher frequencies. Different lengths of elastic band and different points of attachment to the structure were considered to ensure that the suspension did not influence the beam's dynamic characteristics. The beam was excited in the y-direction through the use of an electromagnetic exciter/shaker. A stinger was used to connect the shaker to the force transducer that was mounted on the

beam. Piezoelectric accelerometers were attached at the sensor locations with beeswax.

The layout of the measurement system is shown in Figure 5.2, the core of which is the *DSPT ™ Siglab 24-40*. This piece of equipment performs the role of a signal generator, as well as a data acquisition and processing mechanism and can easily be controlled with a mini-computer. Details of the other components of the measurement system and their calibration can be found in Appendix A.

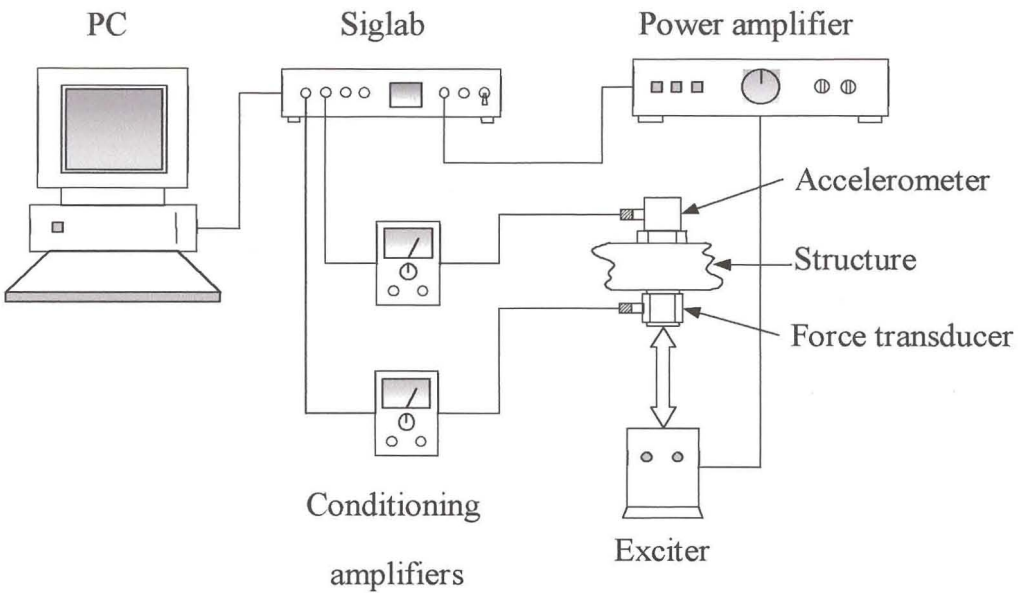

Figure 5.2 – Measurement system used for the identification of a single harmonic force

5.1.2 The Measurements

The test was conducted to cover the chosen range of frequencies from 0 Hz to 500 Hz, which included the first five bending modes. The excitation was applied at position 11, while measuring at 11 response locations with a single roving accelerometer. The excitation point was chosen since it is the only point that properly excites all the modes in the direction of excitation. The accelerometer was small enough so that its inertia loading on the beam was considered negligible.

Inertance frequency response functions were measured for each of the response locations. A lot of time was spent to ensure proper definition of the resonance peaks and anti-resonances. This resulted in changing the excitation point and considering different stinger configurations.

Another factor that influenced the quality of the resonance peaks was the excitation function used in determining the frequency response functions. At first a true random signal was used to excite the structure. The true random excitation violates the periodicity requirement of the FFT process, since neither the force nor the response is periodic within the measurement time. This results in an error known as 'leakage'. The effect of leakage can be reduced by applying a 'window' (typically a Hanning window), but not completely eliminated. The frequency response function is computed by dividing the output spectrum by the input spectrum, and since each spectrum is different, the effect of the convolution (see Section 2.1) does not divide or ratio out. Especially, the peak values in the frequency response function measurements will be influenced by leakage most heavily, and may appear blunt and poorly defined. Furthermore, the coherence function is not unity at the resonances and anti-resonances. Hence, the structure will appear to be more damped than what is actually the case. This is particularly true for lightly damped structures. (Olsen, 1984 and Avitabile, 1999)

In view of the above-mentioned difficulties associated with the true random signal, the chirp-sine function, or swept sine burst, was used instead. This signal satisfies the periodicity requirement and will not experience the 'leakage' phenomenon. The peaks on the frequency response function were much sharper and better defined. There was also an improvement in the coherence function.

The frequency response function is, by definition, the Fourier transform of the system's response divided by the Fourier Transform of the applied force. This relation is only valid if the system is assumed to behave linearly. A linear system will also obey Maxwell's reciprocity theorem, which will yield symmetric mass, stiffness, damping and frequency response function matrices. Since the frequency response function matrix is symmetric, it is theoretically at least possible to determine the entire matrix by simply considering one column (or row) of the frequency response function. To check the reliability of the frequency response function measurements, a second column of the inertance matrix was measured by exciting position seven. Figure 5.3 illustrates the reciprocity check for the beam structure and confirms that the beam behaves linearly.

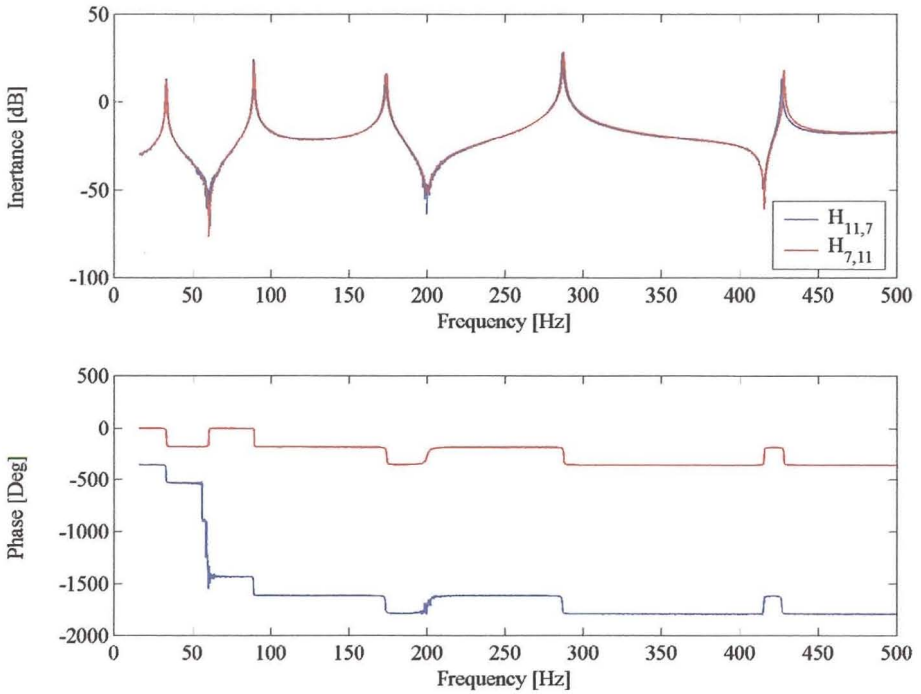

Figure 5.3 – Reciprocity check of frequency response functions for the aluminium beam

The point inertance of the measured frequency response function is presented in Figure 5.4 (the entire set being represented in Appendix B) and exhibits the expected anti-resonance after each resonance.

The beam was then excited with a harmonic forcing function of a 100 Hz. The applied force was measured directly with the force transducer for comparison with the force predictions. The Auto Spectral Densities (ASD) of the acceleration signals corresponding to each sensor location were also measured taking 30 frequency domain averages.

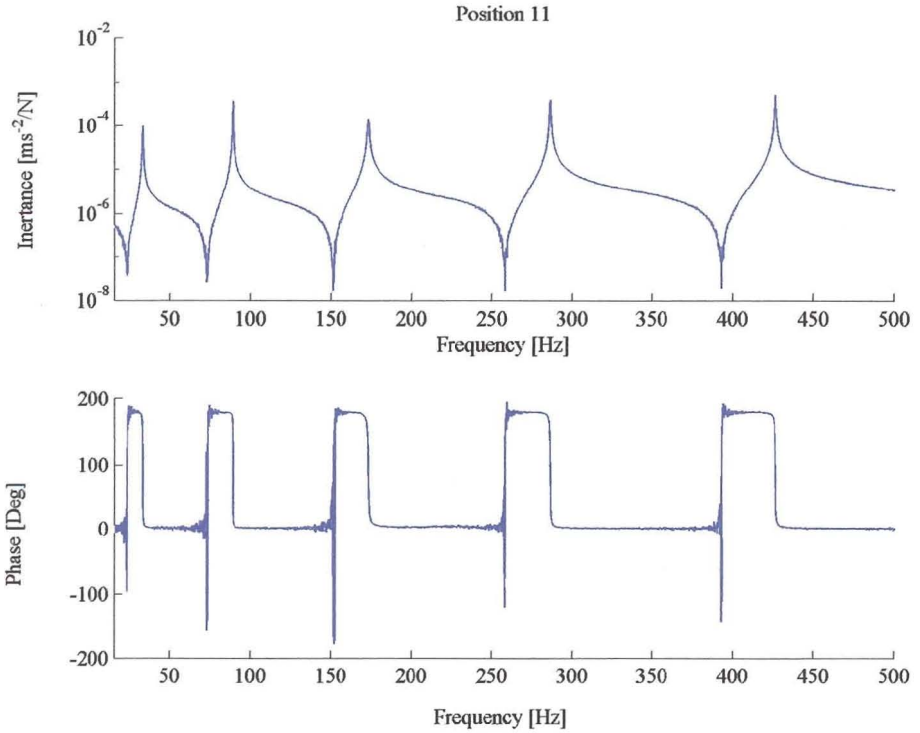

Figure 5.4 – Measured point inertance (position 11) for the free-free beam.

5.1.3 Force Determination Results

a) Frequency Response Function Method

From the measured frequency response functions it is evident that the noise is particularly acute at the anti-resonances. In these regions the response signal tends to become very small and is susceptible to pollution and noise. It was decided to 'smooth' the frequency response functions by performing the experimental modal analysis given in Section 2.3. The RBM were excluded from the analysis, since they were not properly excited and were below the frequency range of the accelerometer and exciter used in the analysis. The point inertance of the measured frequency response function data and the reconstructed normal mode model (residual terms included) are presented in Figure 5.5 (the entire set and modal parameters being represented in Appendix B).

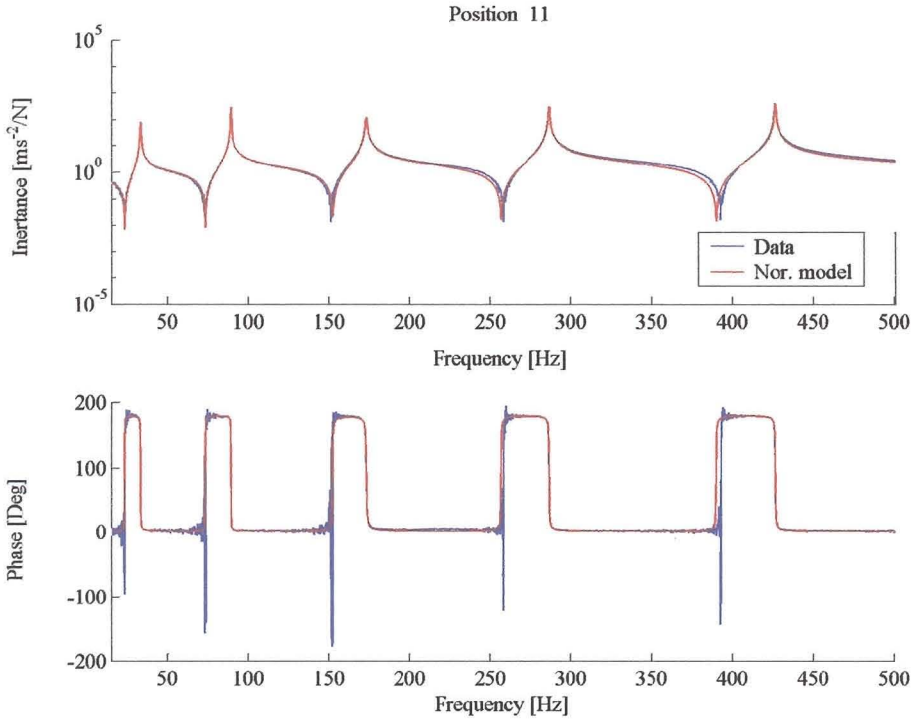

Figure 5.5 – Measured and reconstructed point inertance (position 11) for the free-free beam.

Having measured the frequency response function matrix and the accelerations due to the applied force, the force could be determined from

$$\{\hat{F}(\omega)\} = [A(\omega)]^{+}\{\ddot{X}(\omega)\} \tag{5.1}$$

Only four sensor locations were included in the calculations, these being positions 6, 8, 9 and 11. SVD was used to calculate the pseudo-inverse of the reconstructed frequency response function matrix. The force estimates are shown in Figure 5.6 where they may be compared with the directly measured force. Since we only measured the ASD of the force and responses the terms in equation 5.1 are real, and as a result there is no phase information available.

It is obvious from the results (Figure 5.6) that the frequency response function method accurately identified the single harmonic force acting on the free-free beam, with a FEN of only 0.141 per cent at the excitation frequency.

Increasing the number of response measurements is likely to improve the quality of the force estimate by averaging the errors.

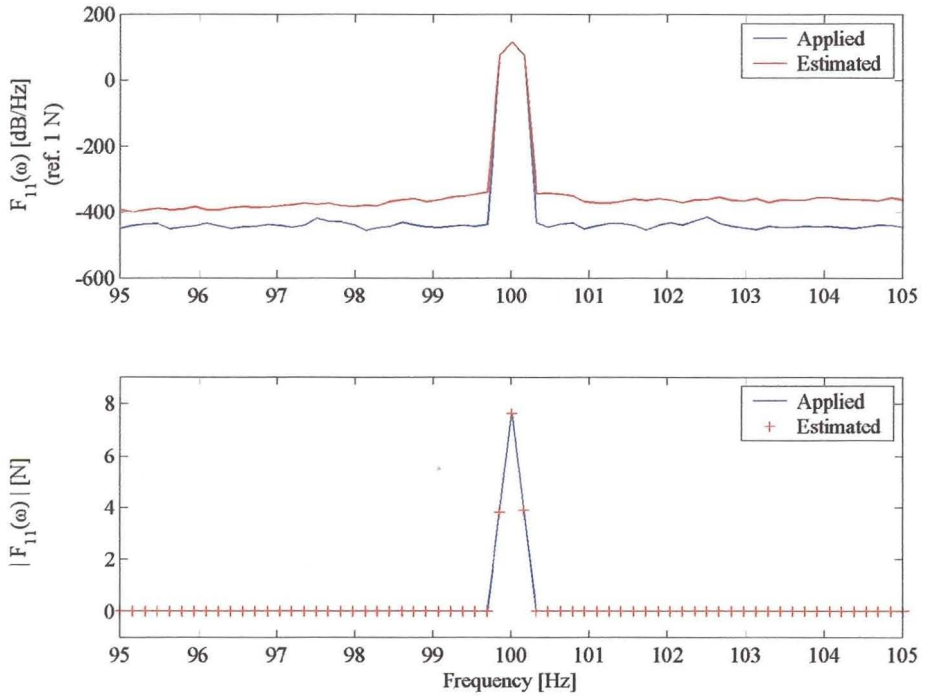

Figure 5.6 – Comparison of the measured and estimated force for free-free beam corresponding to position 11

b) Modal Coordinate Transformation Method

The single harmonic force was calculated from equation (4.16), i.e.

$$\{\hat{F}(\omega)\} = [\Phi^T]^+ [S(\omega)]^{-1} [\Phi]^+ \{X(\omega)\} \tag{5.2}$$

All five modes in the range of frequencies were included in the analysis. This method failed to predict the correct force amplitudes. The source of error may be attributed to poor modal identification, which can be explained as follows:

The formulation of the two frequency domain methods, considered in this work, is essentially the same. Both use the frequency response function to express the relation between the applied force(s) and the associated response. The only difference being the calculation of the pseudo-inverse. In the case of the frequency response function method the pseudo-inverse of the whole frequency response matrix is calculated, while the modal coordinate transformation method considers only the pseudo-inverse of the modal matrix. Thus, while the former allows the incorporation of the residual terms corresponding to the truncated modes, there is no manner in which one can account for these terms in the latter. Figure 5.7 illustrates this point. Here the normal mode model for the free-free beam, with and without the residual

terms, is compared to the originally measured frequency response function. It can be seen that the exclusion of the residual terms has a significant effect on the accuracy of the frequency response function, and subsequently on the success of the modal coordinate transformation method.

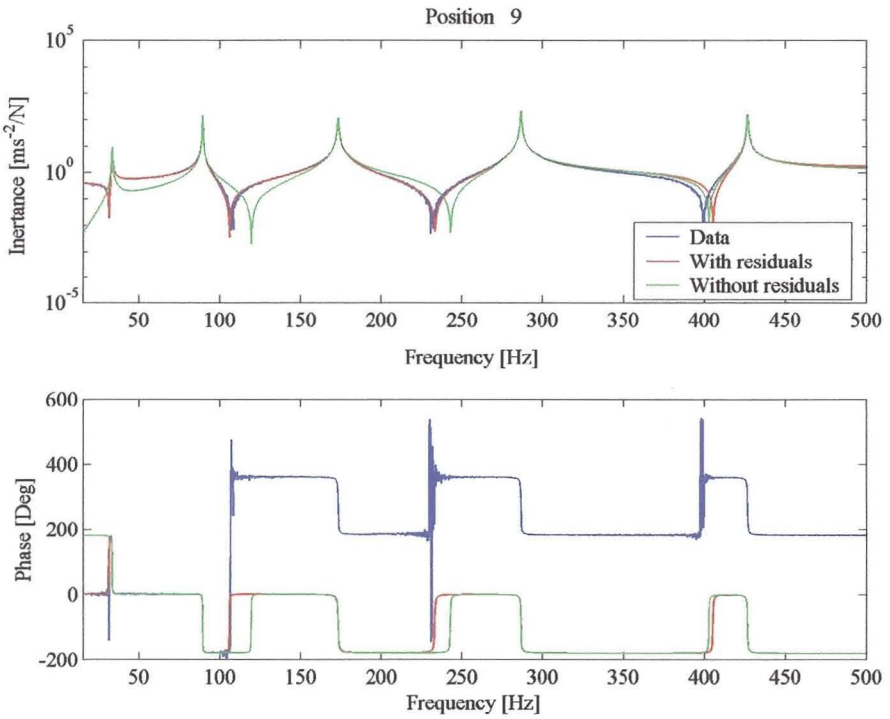

Figure 5.7 – Measured and reconstructed normal mode model of the frequency response function, $A_{9\ 11}(\omega)$ for free-free beam.

A numerical simulation of the free-free beam revealed that the low frequency contribution, i.e. the RBM, had the most adverse affect on the accuracy of the frequency response functions at the excitation frequency (100 Hz).

The implication this has is that the frequency range should consist of the entire modal space of the model. This means that the residual contributions from modes outside the analysis frequency range, which are not represented in the modal matrix, must be small. (Warwick and Gilheany, 1993). As a result one would need to include a larger frequency range in the experimental modal analysis, than the frequency range for which one would like to estimate the forces (Clark *et al.*, 1998).

It is important to note that the frequency response function matrix may either be reconstructed with the residual terms included, as was the situation in the former subsection, or without the residual terms. From here onwards the term -

reconstructed frequency response function - will refer to the case where residual terms are omitted.

5.2 SINGLE HARMONIC FORCE: HINGED-HINGED BEAM

The aim of this section is to ascertain a single harmonic force on a hinged-hinged beam.

5.2.1 Details of the Experimental Set-up

The aluminium beam was fixed at the ends to approximate a hinged-hinged beam (also referred to as a simply supported beam). In theory, at least, this type of constraint will only allow rotations at the supports, while restraining the beam from any translations. However, in practice, this constraint is much more difficult to implement, since the construction of the clamping often causes significant resonance frequency and mode shape differences. Figure 5.8 shows the construction of the supports.

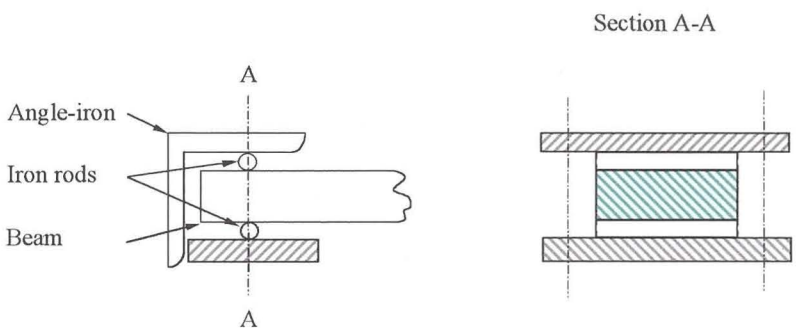

Figure 5.8 – Construction of the support for the hinged-hinged beam

The basic idea was to keep the contact area between the beam and the support as small as possible to allow the beam to rotate about a single point. In order to accomplish this the beam was fastened between two iron rods with a diameter of approximately 5 millimetres. An angle-iron section was placed on top and bolted to concrete-filled blocks.

Although it was the initial intention to approximate a hinged-hinged beam, the dynamic characteristics of the beam may be quite different from those of the theoretical boundary condition. However, no attempt was made to confirm that the imposed boundary conditions satisfied the requirements of that of a hinged-hinged beam. It was assumed that the test boundary conditions matched that of the operating boundary conditions of a specific beam in practice. Having said this, the boundary conditions will still be referred to as hinged-hinged.

The same sensor locations were retained as before, the only difference being the exclusion of positions 1 and 11 from the measurements, since the response of these points were considered to be zero. The sensor locations are depicted in Figure 5.9.

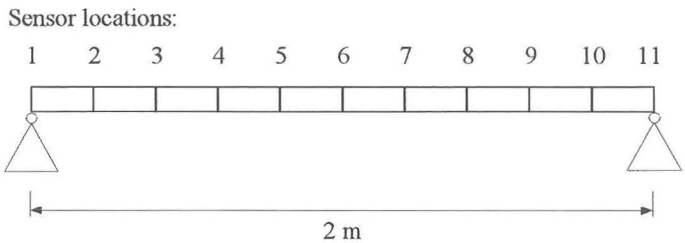

Figure 5.9 – Hinged-hinged aluminium beam and response locations

Since the beam was 'grounded' there are no RBMs contributing to the response of the beam.

The measurement system remained unchanged and was used for measuring frequency response functions, accelerations and force levels.

5.2.2 The Measurements

The test was conducted to cover the chosen range of frequencies from 0 Hz to 500 Hz, which included the first six bending modes. The excitation was applied at position 8, while measuring at nine response locations (sensor location 2 to 10) with two roving accelerometers. The accelerometers were small enough so that their inertia loading on the beam were considered as negligible.

Despite attempts to improve the quality of the frequency response functions through the use of a chirp-sine excitation, the author still experienced difficulties associated with the measured frequency response functions. Especially, when an experimental modal analysis had to be performed on the data to extract the necessary modal parameters the curve-fitting algorithm failed to produce satisfactory results. One of the likely reasons may be attributed to the fact that the beam can be considered as a lightly damped structure, which requires a very small frequency resolution to ensure proper definition of the resonance peaks. The *Structural Dynamics Toolbox*® (Balmès, 1997) identifies the maximum value of the frequency response function plot within a specified frequency band as the natural frequency of that particular mode. Once the natural frequency has been obtained a curve is fitted to the frequency response function plot, originating from the maximum value, to estimate the damping of the mode in question. Failing to properly excite or measure the resonance will result not only in the wrong natural frequency, but also over-estimate the damping values. This is especially acute where the boundary conditions interfere with the resonances. A

thin rubber strip was glued to the one side of the aluminium beam to increase the damping values. This modification definitely improved the definition of the resonance peaks – nicely curved and not spiky (Figure 5.10). Another advantage of the increased damping is the decrease in the condition number due to higher modal overlap, which may prove to be beneficial to the force identification process.

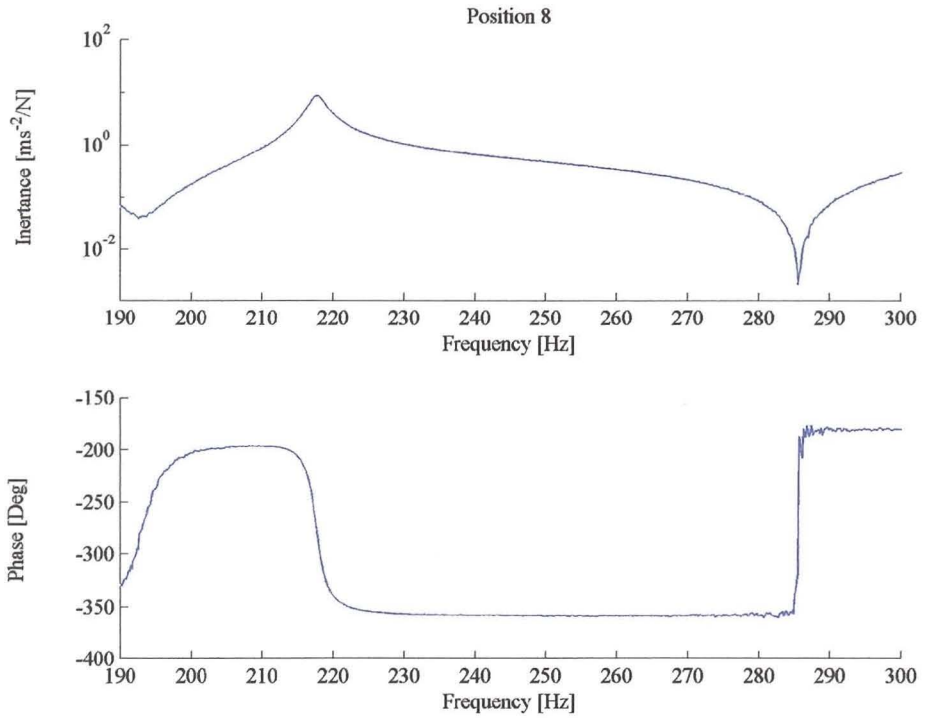

Figure 5.10 – Improvement in the resonance peaks of the point inertance (position 8) due to the attachment of a thin rubber strip.

Inertance frequency response functions were measured for each of the nine sensor locations. Figure 5.11 shows the measured point inertance for the hinged-hinged beam (the entire set being represented in Appendix C).

Successively, the beam was excited with a harmonic forcing function of a 250 Hz, while measuring 30 frequency domain averages of the applied force and acceleration signals.

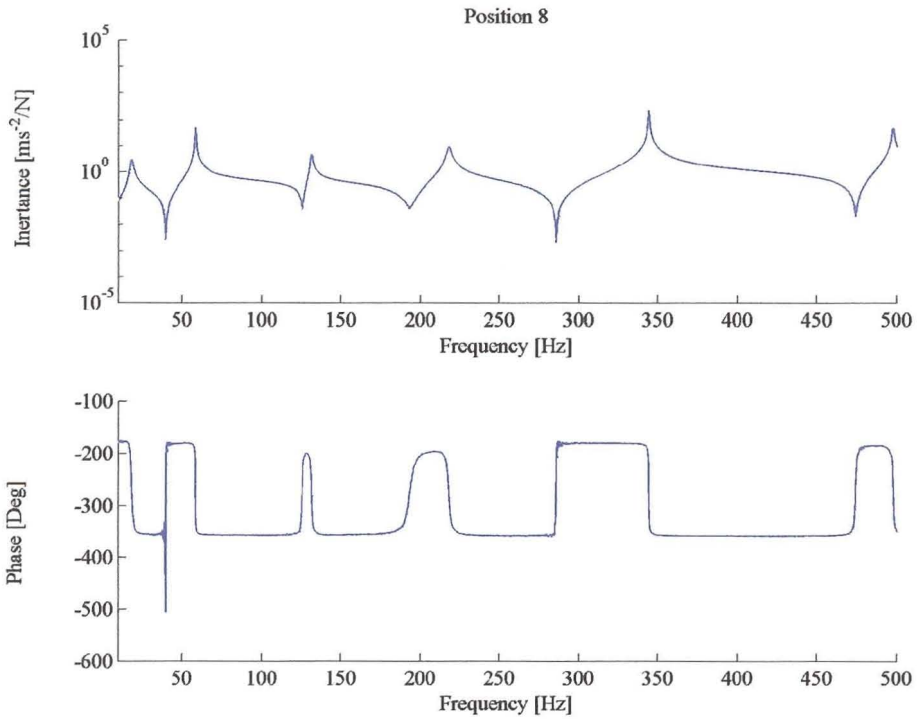

Figure 5.11 – Measured point inertance (position 8) for the hinged-hinged beam.

5.2.3 Force Determination Results

a) Frequency Response Function Method

The actual force may be reconstituted from

$$\{\hat{F}(\omega)\} = [A(\omega)]^{+}\{\ddot{X}(\omega)\} \tag{5.3}$$

by considering only four sensor locations (positions 7, 8, 9 and 10). Unlike the case for the free-free beam the 'raw' frequency response function measurements were used in the force identification process. This resulted in a FEN of 4.202 per cent at 250 Hz and the forces are compared in Figure 5.12.

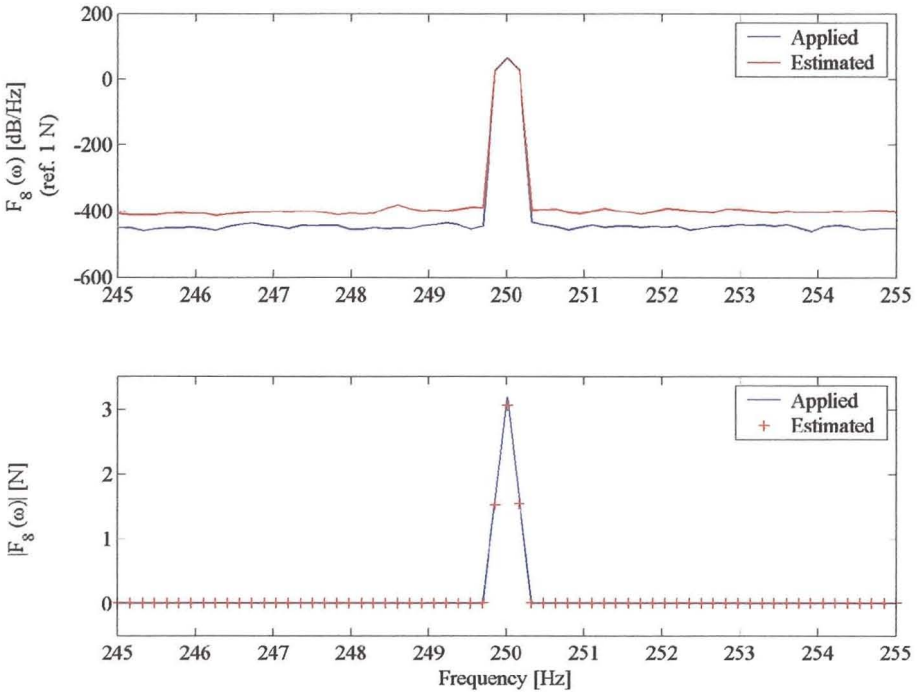

Figure 5.12 – Comparison of the measured and estimated forces for hinged-hinged beam

b) Modal Coordinate Transformation Method

The force estimates were obtained from using equation (5.2). Five modes were included in the analysis. Once again the reconstructed frequency response functions deviated noticeably from the measured values at the excitation frequency. Based on the explanation given in the previous section, in practice one would have no other choice than to increase the frequency range to include more modes, thereby ensuring that the residual contributions from the modes outside the frequency range are small enough. Instead, it was decided to alter the forcing frequency and only repeat the force and response measurements, rather than the laborious frequency response function matrix. The excitation frequency was reduced to a 100 Hz. Six sensor locations (positions 6, 10, 4, 2, 8 and 3) were necessary to obtain acceptable force estimates. These sensor locations were selected from all possible sensor locations with Krammer's effective independent algorithm (refer to Section 4.3.1) and are sorted from most to least important. The force results were presented in Figure 5.13. Interesting to note is that the actual and predicted forces have a much higher noise floor, as a result of a larger frequency resolution applied during the measurements.

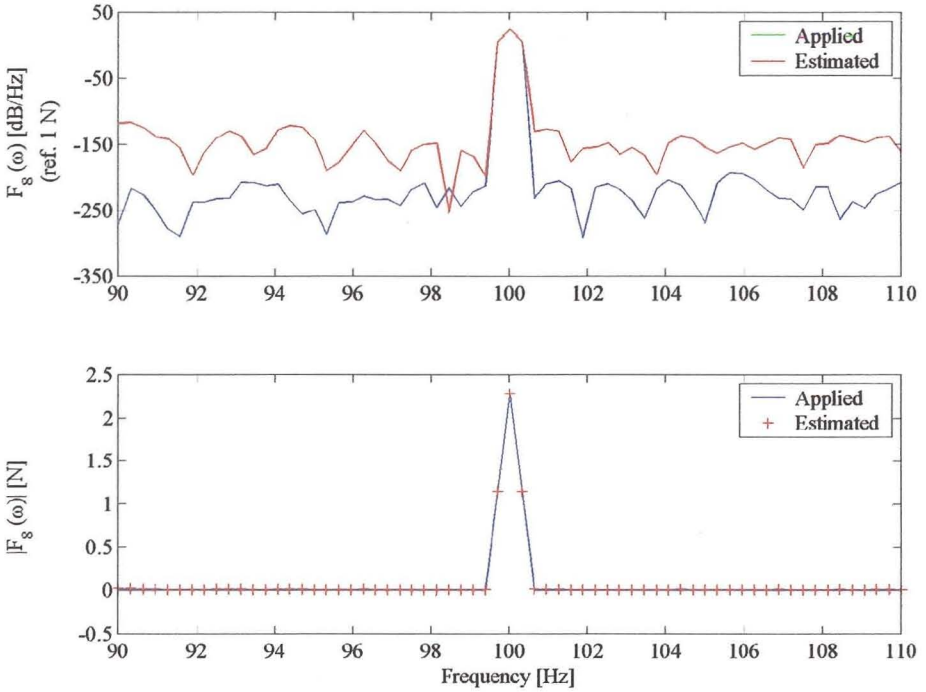

Figure 5.13 - Comparison of the measured and estimated forces for the hinged-hinged beam.

Application of the RMV, outlined in Section 4.4, produced similar results to the pseudo-inverse of the modal matrix, although the former required a lot more computational effort.

The FEN for each case is listed in Table 5.1.

Table 5.1 Force Error Norm of the estimated force

Modal matrix [%]	RMV [%]
5.014	5.048